JNCI J Natl Cancer Inst, 2015, 1–11

doi:10.1093/jnci/dju419
First published online February 6, 2015
Article

ARTICLE

Simultaneous β1 Integrin-EGFR Targeting and Radiosensitization of Human Head and Neck Cancer

Iris Eke, Katja Zscheppang, Ellen Dickreuter, Linda Hickmann, Ercole Mazzeo, Kristian Unger, Mechthild Krause, Nils Cordes

Affiliations of authors: OncoRay, National Center for Radiation Research in Oncology, Faculty of Medicine and University Hospital Carl Gustav Carus, Technische Universität Dresden, Dresden, Germany and Helmholtz-Zentrum Dresden, Rossendorf, Dresden, Germany (IE, KZ, ED, LH, EM, MK, NC); Department of Radiation Oncology, University Hospital Carl Gustav Carus, Technische Universität Dresden, Germany (IE, MK, NC); Institute of Radiopharmaceutical Cancer Research, Helmholtz-Zentrum Dresden, Rossendorf, Dresden, Germany (KZ); Research Unit Radiation Cytogenetics, Helmholtz-Zentrum München, German Research Center for Environmental Health, Neuherberg, Germany (KU); Clinical Cooperation Group "Personalized Radiotherapy in Head and Neck Cancer," Helmholtz-Zentrum München, Neuherberg, Germany (KU); German Cancer Consortium (DKTK), Dresden, Germany, and German Cancer Research Center (DKFZ), Heidelberg, Germany (MK, NC); Institute of Radiooncology, Helmholtz-Zentrum Dresden, Rossendorf, Dresden, Germany (MK, NC).

Correspondence to: Nils Cordes, MD, PhD, OncoRay – National Center for Radiation Research in Oncology, Medizinische Fakultät Carl Gustav Carus, Technische Universität Dresden, Fetscherstrasse 74 / PF 41, 01307 Dresden, Germany (e-mail: nils.cordes@oncoray.de).

Abstract

Background: Signaling from integrins and receptor tyrosine kinases (RTKs) contributes substantially to therapy resistance of malignant tumors. We investigated simultaneous β1 integrin-epidermal growth factor receptor (EGFR) targeting plus radiotherapy in human head and neck squamous cell carcinomas (HNSCCs).

Methods: Ten HNSCC cell lines were grown in three-dimensional laminin-rich extracellular matrix cell cultures and two of them as tumor xenografts in nude mice (n = 12–16 per group). Targeting of β1 integrin and EGFR with monoclonal inhibitory antibodies (AIIB2 and cetuximab, respectively) was combined with x-ray irradiation. Clonogenic survival, tumor growth, and tumor control (evaluated by Kaplan-Meier analysis), apoptosis, phosphoproteome (interactome, network betweeness centrality analysis), receptor expression (immunohistochemistry), and downstream signaling (western blotting) were assessed. Various mutants of the integrin signaling mediator focal adhesion kinase (FAK) were employed for mechanistic studies. All statistical tests were two-sided.

Results: Compared with β1 integrin or EGFR single inhibition, combined β1 integrin-EGFR targeting resulted in enhanced cytotoxicity and radiosensitization in eight out of 10 tested HNSCC cell lines, which responded with an FAK dephosphorylation after β1 integrin inhibition. In vivo, simultaneous anti-β1 integrin/anti-EGFR treatment and radiotherapy of UTSCC15 responder xenografts enabled better tumor control compared with anti-EGFR monotherapy and irradiation (hazard ratio [HR] = 6.9, 95% confidence interval [CI] = 1.6 to 30.9, $P = .01$), in contrast to the SAS nonresponder tumor model (HR = 0.9, 95% CI = 0.4 to 2.3, $P = .83$). Mechanistically, a protein complex consisting of FAK- and Erk1-mediated prosurvival signals for radiation resistance, which was effectively compromised by β1 integrin and EGFR blocking.

Conclusions: Concomitant targeting of β1 integrin and EGFR seems a powerful and promising approach to overcome radioresistance of HNSCCs.

Received: July 15, 2014; **Revised:** November 10, 2014; **Accepted:** November 11, 2014

Tumor cell resistance to therapy evolves from genetic and epigenetic modifications, as well as microenvironmental cues severely hampering local tumor control and cure (1–3). Current concepts seek optimized tumor cell eradication through specific targeting of central prosurvival signaling molecules (4–7). cetuximab blocking of the epidermal growth factor receptor (EGFR) is the prime example of a molecular approach successfully transferred into improved cure rates of patients with head and neck squamous cell carcinomas (HNSCCs) (8). In line with receptor tyrosine kinase (RTK) targeting, cell surface integrin receptors emerged as promising cancer targets (9–13).

EGFR is a member of the ErbB family of RTK and frequently hyperactive and/or overexpressed in human neoplasias (14). Via auto- and paracrine stimulation, EGFR dimerization and autophosphorylation initiates mitogenesis and migration predominantly through Ras-Extracellular signal-regulated kinase (Erk), AKT and c-Jun NH2-terminal kinase (JNK) cascades (14). Because of this multifunctionality and promising preclinical data in various tumor types from, for example, head and neck, lung, and colon (15–20), EGFR emerged as potent cancer target (21,22). For further therapy optimization, prosurvival bypass signaling induced by anti-EGFR therapeutics and mutual, cooperative interactions between EGFR and other transmembrane receptors requires investigation (17,23,24).

Such interactions are documented for β1 integrin and EGFR (18,25–27). Similar to EGFR, β1 integrin overexpression is found in a variety of human malignancies including HNSCC (28,29), in which this integrin serves as strong determinant of tumor therapy resistance (30). While clinical trials evaluating β1 integrin antagonist monotherapy (http://clinicaltrials.gov/ct2/results?term=integrin&pg=1) are still ongoing, targeting of β1 integrin has demonstrated strong potential in preclinical studies to sensitize cancer cells to conventional radio- and chemotherapies (31–33). Generally, the 24 known integrin receptors consist of an α and a β subunit and contribute to the regulation of cell survival, proliferation, and invasion (10,11,34–37).

Without intrinsic kinase activity, integrins recruit cytoplasmic signaling molecules and adapter proteins to their cytoplasmic tail for signaling (38). Predominantly, focal adhesion kinase (FAK) but also Erk and AKT signaling cascades channel biochemical information from β1 integrins and EGFR (27,39,40). Upon activation of β integrins or growth factor receptors, Tyrosine (Y)397 of FAK is autophosphorylated (40) and facilitates functions in cell motility, proliferation, and the stress response to ionizing radiation and chemotherapy (33,41–43). FAK is frequently overexpressed and hyperphosphorylated in various cancers originating, for example, from liver (44), breast (45), and head and neck (46).

On the basis of intrinsic and acquired therapy resistance promoted by EGFR and β1 integrin overexpression, we investigated the potential of simultaneous targeting of EGFR and β1 integrin for radiosensitization of HNSCC in vitro and in vivo. We demonstrate that HNSCC cells susceptible for β1 integrin targeting show cross-susceptibility for EGFR inhibition resulting in radiosensitization. Mechanistically, prosurvival FAK and Erk signaling are more efficiently hampered upon combined anti-β1 integrin/anti-EGFR treatment than either treatment alone. Thus, the prominent function of EGFR and β1 integrin in HNSCC can be exploited for improved tumor control and reduced radioresistance.

Methods

Cell Cultures, Antibody Treatment, Radiation Exposure, and siRNA Knockdown

Human squamous cell carcinoma cell lines (UTSCC45, UTSCC15, UTSCC14, UTSCC8, UTSCC5, SAS, Cal33, FaDu, HSC4, XF354) of the head and neck (HNSCC) were used. The origin and stability of the cells were routinely monitored by short tandem repeat analysis (microsatellites). To accomplish three-dimensional growth, cells were imbedded in a laminin-rich extracellular matrix (lrECM; Matrigel, BD) as published (17,33). Further details about cell culture conditions, cell treatment, growth conditions, and siRNA sequences are described in the Supplementary Methods (available online).

Total Protein Extracts, Western Blotting, and Phosphoprotein Microarray Analysis

Three-dimensional cell cultures were treated with AIIB2, cetuximab, or both or IgG isotype control for one hour. Cell harvesting, whole cell lysates, SDS-PAGE, and western blotting including specific antibodies used were described previously (33). The Phospho Explorer Antibody Microarray was conducted by Full Moon BioSystems Inc., as published (17). Further technical details are described in the Supplementary Methods (available online).

Immunoprecipitation

Immunoprecipitation assays were performed as published (33,47). In brief, Protein G Agarose beads (Sigma) were incubated with specific antibodies over night at 4°C. Beads were washed with 1xPBS prior to incubation with 250 µL 3D lysates (cell lysis buffer, cell signaling) for 24 hours at 4°C. After immunoprecipitates were washed, sample buffer was added to the beads. Evaluation of coprecipitation was performed by SDS-PAGE.

Mass Spectrometric Analysis

To identify FAK-interacting proteins, mass spectrometric analysis was carried out at the Max Planck Institute of Molecular Cell Biology and Genetics Mass Spectrometry (MPI-CBG MS) Facility (Dresden, Germany) and performed as published (33,47) and described in the Supplementary Methods (available online).

Proximity Ligation Assay

Proximity ligation was performed according to the manufacturer's protocol and as recently described (33) using the Duolink Detection Kit with PLA PLUS and MINUS probes for mouse and rabbit (Olink Bioscience). Samples were analyzed with Axiovert Z1 observer microscope (Carl Zeiss, Inc.) using a 40x objective.

3D Colony Formation Assay

Clonogenic survival was measured as published (33). Briefly, 96 well plates were coated with 1% agarose, and cells were seeded in lrECM, mixed with culture medium to a final concentration of 0.5 µg/µL. After 24 hours, cells were treated with AIIB2, cetuximab, or AIIB2+cetuximab (IgG isotype as antibody as control) for 24 hours and then irradiated (0–6 Gy). Cell clusters with a minimum of 50 cells were counted microscopically eight to 14 days later, cell line dependently.

In Vivo Experiments

All animal facilities and experiments have been approved by the Landesdirektion Dresden (Dresden, Germany) according to the German and Saxony animal welfare regulations. Immunocompromised seven- to 14-week-old male and female NMRI (nu/nu) mice (Experimental Centre of the Faculty of

Medicine Carl Gustav Carus, Technische Universität Dresden) were further immunosuppressed by whole body irradiation one to five days before tumor transplantation. Cryopreserved UTSCC15 or SAS tumor pieces were serially transplanted onto the backs of mice, as published (15). Tumor cell transplantation, treatment of animals, histology, and protein expression analysis are described in detail in the Supplementary Methods (available online).

Detection of DNA Double Strand Breaks

For the detection of residual DNA double strand breaks (DSB), the S139-phosphorylated H2AX (γH2AX)/p53 binding protein-1 (p53BP1) foci assay was used (48), described in the Supplementary Methods (available online).

FAK Expression Constructs, FAK Site-Directed Mutagenesis and Transfection of FAK Plasmids

Site-directed mutagenesis and stable transfection of FAK plasmids were performed as described (33,49). Mouse FAK wild-type (wt) fragments were amplified by polymerase chain reactoin (PCR) from expression plasmids kindly provided by D. D. Schlaepfer (University of California, San Diego, CA) and inserted into pEGFP-N1 (Clontech). The FAK activation loop was mutated using QuikChange II Site-Directed Mutagenesis Kit (Stratagene) according to manufacturer's instructions. Cells were stably transfected using lipofectamine (Invitrogen) and selected with G418 (Calbiochem) for four weeks.

Bioinformatics and Network Analysis

The processing and bioinformatics analysis of the protein microarray data sets provided by Full Moon BioSystems Inc. are described in detail in the Supplementary Methods (available online).

Statistical Analysis

Data are presented as mean ± SD of at least three independent experiments. Values of the radiation survival curves were transformed to a logarithmic scale before Student's *t* test analysis was performed. Data points with zero colonies were replaced with 0.5 colonies to enable logarithmic transformation. The level of significance was determined by unpaired, two-sided Student's *t* test and Mann-Whitney U test (median values for tumor growth time) using Microsoft Excel 2003. For in vivo tumor control curves, log-rank test (actuarial estimates for time to local tumor recurrence were obtained using the Kaplan-Meier method; GraphPad Prism software version 4.03) was used. Results were considered statistically significant if a *P* value of less than .05 was reached.

Results

β1 Integrin Inhibition and Activation of EGFR-Associated Signaling in HNSCC

β1 integrin targeting mediates substantial cytotoxicity and enhanced radiosensitivity in various cancer models. Whether such a treatment cross-activates prosurvival bypass signaling was tested by phosphoproteome array technology. We found hyperphosphorylated B-Raf Serine (S)602 (fold change 2.01) and P70S6K Threonine (T)421 (fold change 1.83) and less phosphorylated MEK1 T286 (fold change 0.59) after siRNA-mediated β1 integrin depletion (Figure 1A). Confirmatory data were generated with β1 integrin-inhibitory antibody AIIB2 in 3D HNSCC cell cultures and tumor xenografts, and it was demonstrated that Erk1/2 phosphorylation was also elevated in vitro (fold change 1.78±0.53, $P = .06$) as well as in vivo (fold change 1.20±0.03, $P < .001$) (Figure 1, B and C). To identify a mechanistic link between EGFR and β1 integrin pathways, we performed mass spectrometry on FAK immunoprecipitates and found Erk1 and MEK1 (Figure 1D; Supplementary Table 1). Importantly, β1 integrin deactivation induced dissociation of the FAK-Erk1 protein complex (Co IgG: 55.13±8.01 interactions/cell; AIIB2: 14.00±4.43 interactions/cell, $P = .002$) (Figure 1E) indicating a physical connection between both molecules (Figure 1, D and E). These data suggest that β1 integrin blocking elicits EGFR-related bypass downstream signaling involving FAK-Erk1/2 interactions.

Combined β1 Integrin/EGFR Targeting and Its Effect on Radiosensitivity and Tumor Control

We proceeded with evaluating the cytotoxicity and radiosensitivity of cetuximab on top of AIIB2 to inhibit AIIB2-mediated prosurvival signaling (Figure 2, A-D). Intriguingly, monotherapies of AIIB2 and cetuximab as well as combined β1 integrin/EGFR inhibition caused substantial cytotoxicity in nine out of 10 β1 integrin- and EGFR-expressing HNSCC cell lines (surviving fraction AIIB2+cetuximab: XF354: 0.15±0.13, $P < .001$; UTSCC14: 0.09±0.05, $P < .001$; Cal33: 0.19±0.04, $P < .001$; UTSCC45: 0.57±0.12, $P = .003$; UTSCC8: 0.12±0.07, $P < .001$; UTSCC5: 0.39±0.12, $P < .001$; UTSCC15: 0.67±0.04, $P < .001$; HSC4: 0.66±0.11, $P < .001$; FaDu: 0.63±0.08, $P = .001$; SAS: 0.65±0.21, $P = .05$) (Figure 2, A and C; Supplementary Figure 1, A and B, available online), which was accompanied by elevated Caspase 3 cleavage (Supplementary Figure 2, A-C, available online). Regarding radiosensitization, simultaneous AIIB2/cetuximab administration was superior to single AIIB2 or cetuximab treatment in eight out of 10 HNSCC cell lines for example in Cal33 (surviving fraction 6 Gy: Co IgG: 0.12±0.01; AIIB2: 0.04±0.01, $P = .001$; cetuximab: 0.07±0.02, $P = .02$; AIIB2+cetuximab: 0.01±0.01, $P = .007$), UTSCC45 (surviving fraction 6 Gy: Co IgG: 0.07±0.02; AIIB2: 0.03±0.001, $P = .008$; cetuximab: 0.04±0.01, $P = .03$; AIIB2+cetuximab: 0.01±0.01, $P = .007$), and UTSCC15 (surviving fraction 6 Gy: Co IgG: 0.31±0.03; AIIB2: 0.15±0.005, $P < .001$; cetuximab: 0.18±0.004, $P < .001$; AIIB2+cetuximab: 0.05±0.01, $P < .001$), and in contrast to the two nonresponder cell lines FaDu (surviving fraction 6 Gy: Co IgG: 0.16±0.03; AIIB2: 0.12±0.05, $P = .29$; cetuximab: 0.11±0.07, $P = .26$; AIIB2+cetuximab: 0.08±0.03, $P = .03$) and SAS (surviving fraction 6 Gy: Co IgG: 0.35±0.18; AIIB2: 0.34±0.19, $P = .90$; cetuximab: 0.39±0.23, $P = .97$; AIIB2+cetuximab: 0.34±0.18, $P = .96$) (Figure 2D). Interestingly, these findings were not associated with target expression (Supplementary Figure 3, A and B, available online). Supportive of these data was the number of residual double strand breaks (rDSBs), which was statistically significantly higher and accompanied by impaired DNA-PK S2609 phosphorylation upon single or combined AIIB2/cetuximab plus radiotherapy relative to IgG controls (Supplementary Figure 4, A-D, available online).

In tumor xenografts with evident membranous β1 integrin and EGFR colocalization (Figure 3, A-C), targeting β1 integrin (UTSCC15: hazard ratio [HR] = 1.0, 95% CI = 0.4 to 2.4, $P = .94$; SAS: HR = 2.8, 95% CI = 1.2 to 6.6, $P = .02$), or EGFR (UTSCC15: HR = 3.1, 95% CI = 1.4 to 7.2, $P = .007$; SAS: HR = 22.0, 95% CI = 8.7

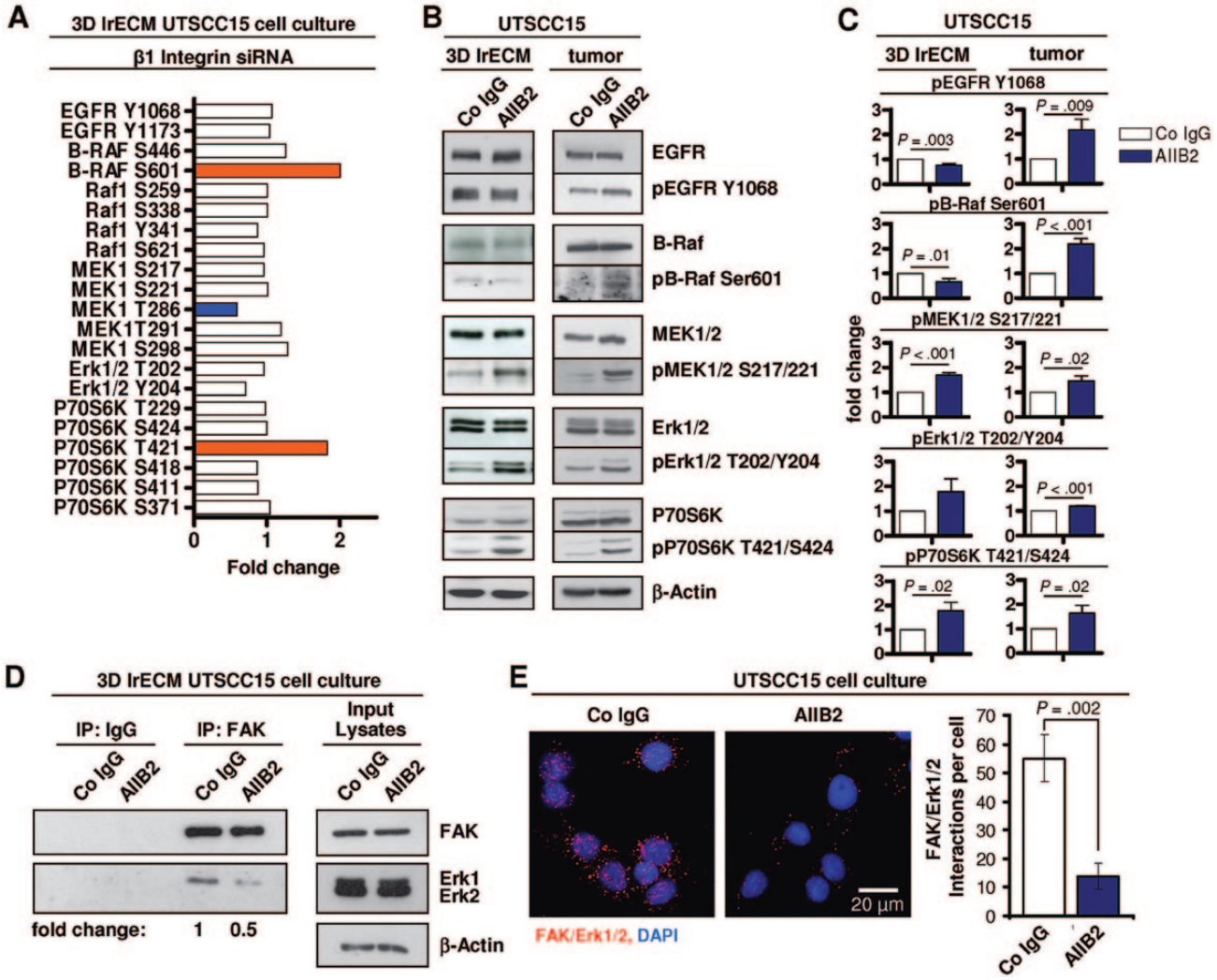

Figure 1. β1 integrin inhibition leads to an activation of the MEK/Erk pathway in human head and neck squamous cell carcinoma cells. **A)** Phosphoproteome array data of 3D-cultured UTSCC15 cells after siRNA-mediated knockdown of β1 integrin. Nonspecific siRNA was used as control. **B)** Western blotting and **(C)** densitometric analysis of UTSCC15 cells after a one-hour treatment with AIIB2 (10 μg/mL) or nonspecific IgG and of homogenates from UTSCC15 xenografts upon AIIB2 (10 mg/kg) or IgG treatment. β-Actin served as loading control. Results show mean ± SD (n = 3, two-sided *t* test). **D)** Western blot analysis of focal adhesion kinase (FAK) and Erk1/2 expression on FAK immunoprecipitates. FAK immunoprecipitation was done from whole cell lysates of AIIB2- or IgG-treated cells. **E)** Proximity ligation assay using FAK and Erk1/2 antibodies in cells treated with AIIB2 (IgG as control). Images were obtained with a confocal microscope. Nuclear staining was performed with DAPI. **Scale bar** = 20 μm. Results show mean ± SD (n = 3, two-sided *t* test). lrECM = laminin-rich extracellular matrix.

to 56.1, $P < .001$), plus radiotherapy showed statistically significant and model-dependent higher tumor control rates in Kaplan-Meier analysis compared with mice treated with nonspecific IgG (Figure 3C). Strikingly, the combined AIIB2/cetuximab/radiotherapy, but not the cetuximab/radiotherapy approach, led to complete cure of mice bearing UTSCC15 tumors (HR = 6.9, 95% CI = 1.6 to 30.9, $P = .01$). In contrast, this triple therapy showed no statistically significant improvement of local tumor control compared with radiation with cetuximab in SAS tumors (HR = 0.9, 95% CI = 0.4 to 2.3, $P = .83$) (Figure 3C). Concordantly, DSB rate and magnitude were in line with the therapeutic outcome in UTSCC15 responders vs SAS nonresponders (Supplementary Figure 5, A and B, available online). These observations evidently show that concomitant EGFR/β1 integrin blocking is superior to single anti-β1 integrin treatment in transmitting cytotoxicity, radiosensitization, and tumor control in HNSCC models responding to AIIB2-mediated β1 integrin inhibition.

Interactome Analysis on Deregulated Phosphoproteins Upon Simultaneous EGFR/β1 Integrin Inhibition and Network Betweeness Centrality Analysis

Key changes in the intracellular signaling network were identified using antibody-based phosphoproteome arrays covering 1358 phospho-sites of 581 proteins. The complete panel of specific phosphorylations in β1 integrin/EGFR-depleted cells is shown in Supplementary Table 2 (available online). In total, four phosphoproteins were upregulated under β1 integrin depletion, three downregulated and 30 upregulated under EGFR depletion, five downregulated and 17 upregulated under EGFR/β1 integrin depletion, and 16 either up- or downregulated in all three depletion groups. An interaction map of deregulated proteins was built on the 2012 Reactome database (50) using the Cytoscape (51) (www.cytoscape.org) FI plugin. The visualized interaction networks consisted of four nodes (proteins) representing β1

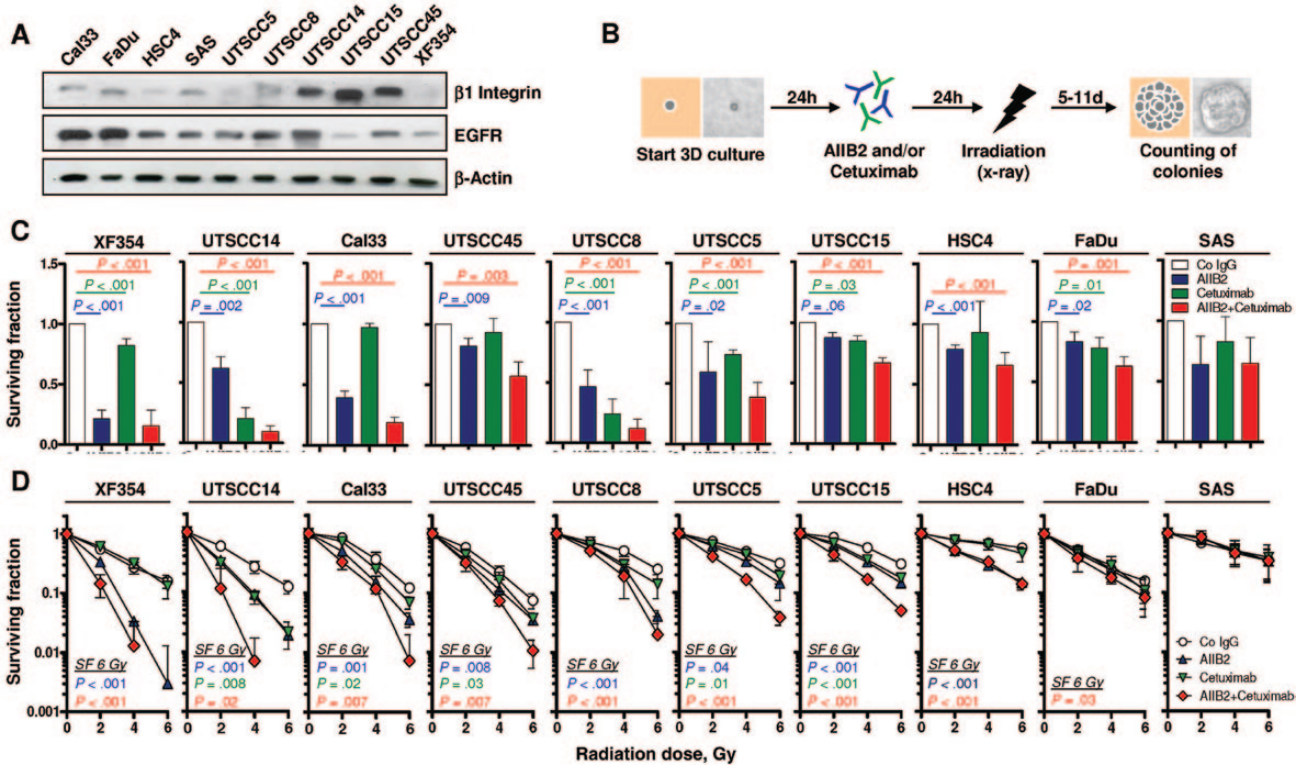

Figure 2. Combined β1 integrin/estrogen growth factor receptor (EGFR) inhibition results in enhanced cytotoxicity and radiosensitization. **A)** Western blot analysis of β1 integrin and EGFR in human head and neck squamous cell carcinoma cell lines. β-Actin served as loading control. **B)** Work flow of colony formation assay of 3D laminin-rich extracellular matrix (lrECM) cell cultures upon AIIB2 or/and cetuximab treatment with or without x-ray irradiation. **C)** Clonogenic survival of 3D cell cultures upon AIIB2 or cetuximab administration (nonspecific IgG as control) (mean ± SD, n = 3, two-sided *t* test). **D)** Clonogenic radiation survival (0–6 Gy, mean ± SD, n = 3, two-sided *t* test) of 24-hour AIIB2 and/or cetuximab-pretreated 3D lrECM cell cultures (nonspecific IgG as control). *P* values compare surviving fractions (SFs) after 6 Gy upon treatment with AIIB2 vs control IgG (**blue**), cetuximab vs control IgG (**green**), or AIIB2 plus cetuximab vs control IgG (**red**). EGFR = epidermal growth factor receptor.

integrin inhibition, 31 nodes representing EGFR inhibition, 19 nodes of EGFR/β1 integrin inhibition, and 13 nodes representing proteins that were deregulated in all three depletion groups relative to controls (Figure 4A).

The potential impact of dual EGFR/β1 integrin inhibition on focal adhesion signaling was identified by generating an interaction network of deregulated phosphoproteins with the focal adhesion network (as defined by KEGG, hsa04510 [52]) (Figure 4, B and C). Remarkably, the majority of phosphoproteins involved in FAK signaling were upregulated. However, three out of the four most downstream phosphoproteins (CyclinD1, Raf1, MAP2K1) were downregulated. FOXO1, the forth protein that links FAK signaling to apoptosis was upregulated.

Whether the higher degree of radiosensitization through combined EGFR/β1 integrin targeting is reproducible at the network level was measured by mean betweeness centrality of each of the networks. Betweeness centrality (BC) is a so-called centrality measure in graphic network theory representing the "importance" of nodes within the whole network (53). BC is a measure calculated for each node separately and is the number of shortest connections from all nodes to all others in the network that pass through that node. The higher the BC, the more central/important is the node for the network. For this purpose, we matched the phosphoproteins of each network with the complete functional human interaction network (Reactome) and calculated the absolute betweeness centrality of all nodes. When comparing the mean BCs of each treatment network, the double β1 integrin/EGFR depletion showed the highest mean BC (BC = 209263), followed by EGFR (BC = 158135), or β1 integrin (BC = 59685) single depletion (Figure 4D). These measures indicated a stronger perturbation of signaling upon simultaneous β1 integrin/EGFR inhibition than upon single EGFR or β1 integrin targeting (Figure 4D). Hence, this analysis clearly pictures the connection between signaling network modifications and the potential for radiosensitization mediated by a specific receptor inhibition.

Prosurvival Bypass Signaling Upon Combined β1 Integrin/EGFR Targeting

We continued by verifying the phosphoproteome data from knockdown conditions with the antibodies AIIB2 and cetuximab and found similar results regarding the prevention of AIIB2-induced hyperphosphorylation of Raf-MEK1/2-Erk1/2 and FAK signaling by simultaneous AIIB2/cetuximab application in vitro and in vivo (Figure 5, A-D; Supplementary Figure 6A, available online). Moreover, most of the investigated protein candidates showed stronger dephosphorylation levels upon combined therapy than monotherapy. In the nonresponder model SAS, modifications in these kinases were either less pronounced (P70S6K, Erk1/2, FAK) or absent (EGFR, B-Raf, MEK1/2) (Figure 5, C and D; Supplementary Figure 6B, available online). These findings pinpoint the superiority of simultaneous β1 integrin/EGFR targeting for signal transduction blockade, cytotoxicity, and radiosensitization over monotherapy.

The Role of FAK for the Cytotoxicity and Radio sensitization of Combined β1 Integrin/EGFR Targeting

Interestingly, FAK Y397 autophosphorylation was diminished upon both β1 integrin and EGFR targeting, giving rise to the

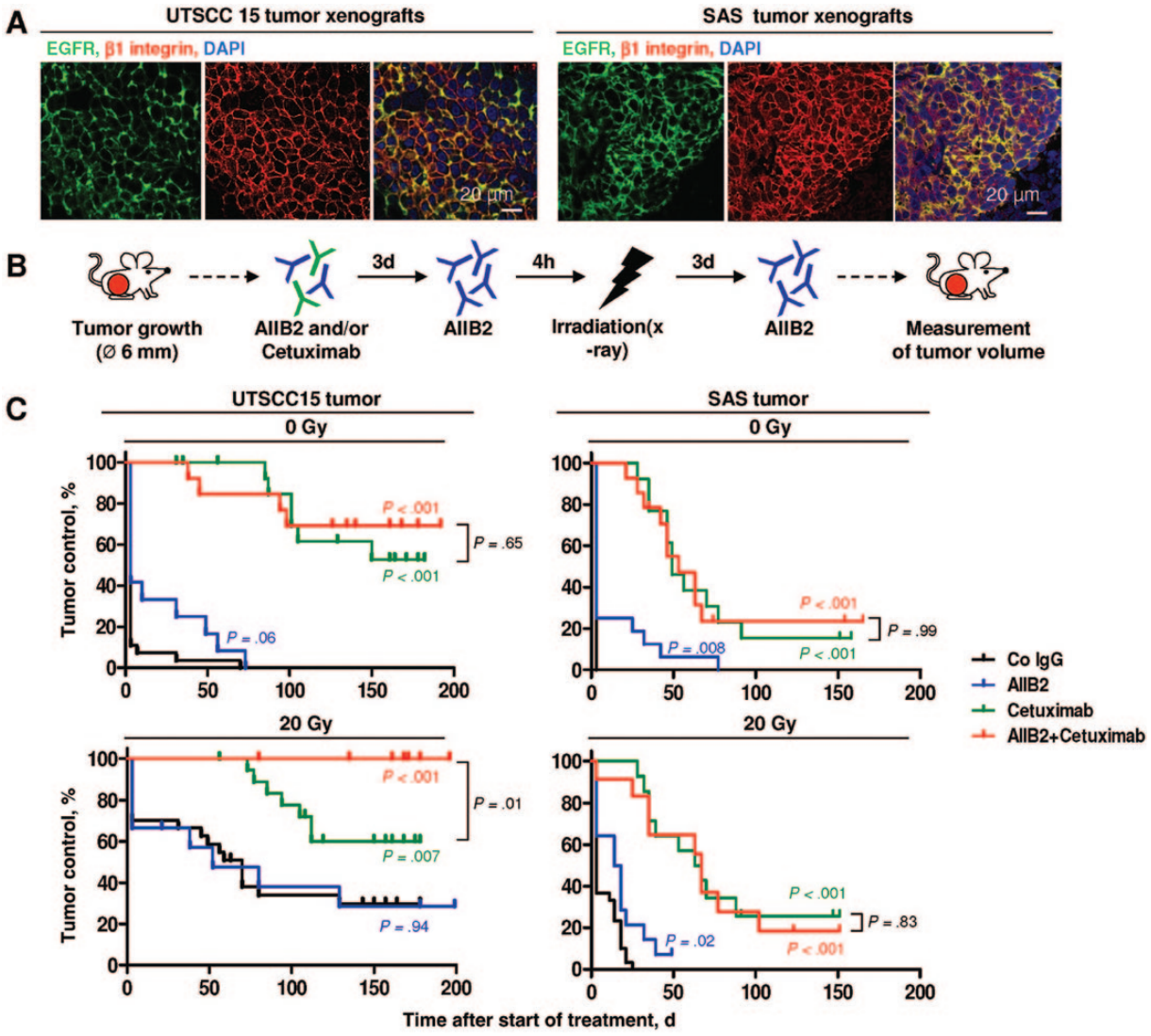

Figure 3. Dual targeting of β1 integrin and epidermal growth factor receptor (EGFR) increases the tumor control of human head and neck squamous cell carcinomas in vivo. **A)** Immunofluorescence staining for β1 integrin and EGFR in UTSCC15 and SAS xenografts. Representative images are shown. **Scale bar** = 20 µm. **B)** Experimental in vivo setup. Subcutaneous UTSCC15 and SAS tumors were grown in immunocompromised mice. Mice (n = 12–16 per treatment group) received three antibody injections of AIIB2 (day 0, 3, 6) or/and one antibody injection of cetuximab (day 0). Where indicated, 20 Gy x-ray radiation was applied four hours after second antibody injection of AIIB2. **C)** Tumor control probability of UTSCC15 and SAS xenografts treated with AIIB2 and/or cetuximab with or without irradiation of 20 Gy is plotted against treatment time. PBS- or IgG-treated xenografts served as controls. *P* values were calculated using the two-sided log-rank test and compare tumor control upon treatment with AIIB2 vs control IgG (**blue**), cetuximab vs control IgG (**green**), AIIB2 plus cetuximab vs control IgG (**red**), and AIIB2 plus cetuximab vs cetuximab (**black**).

question of what critical function FAK plays downstream of these receptors and in connection with their interacting partner Erk1. Strikingly, basal survival was FAK dependent (surviving fraction AIIB2+cetuximab: UTSCC15 GFP: 0.75 ± 0.03, $P < .001$; UTSCC15 FAKwt: 0.87 ± 0.03, $P = .002$; UTSCC15 FAKca: 0.96 ± 0.05, $P < .22$) (Figure 6A), and exogenous overexpression of a constitutively active form of FAK (FAKca) (surviving fraction 6 Gy: Co IgG: 0.48 ± 0.10; AIIB2: 0.46 ± 0.11, $P = .83$; cetuximab: 0.50 ± 0.09, $P = .77$; AIIB2+cetuximab: 0.46 ± 0.07, $P = .89$) completely abrogated the radiosensitizing effects by AIIB2 and cetuximab cells relative to FAK wild-type (wt)–expressing cells (surviving fraction 6 Gy: Co IgG: 0.50 ± 0.06; AIIB2: 0.24 ± 0.04, $P = .003$; cetuximab: 0.30 ± 0.02, $P = .004$; AIIB2+cetuximab: 0.12 ± 0.01, $P = .001$) and GFP vector controls (surviving fraction 6 Gy: Co IgG: 0.25 ± 0.04; AIIB2: 0.11 ± 0.02, $P = .003$; cetuximab: 0.15 ± 0.004, $P = .005$; AIIB2+cetuximab: 0.05 ± 0.02, $P = .004$) (Figure 6B). Interestingly, this FAKca-dependent radiation survival advantage was reflected in the unchanged number of rDSB under AIIB2/cetuximab exposure relative to irradiated FAKwt and GFP control cells (Supplementary Figure 7, available online). Thus, FAK seems highly critical for the DNA damage and survival response controlled by β1 integrin and EGFR.

Our finding that MEK and Erk are dephosphorylated upon AIIB2/cetuximab application, suggesting FAK to function downstream of MEK1/2 and Erk1/2, led us to identify the hierarchical position of FAK within the FAK/Erk1 protein complex (Figure 6, C-F). Single and simultaneous FAK and Erk1 depletion diminished clonogenic survival by approximately 50% (surviving fraction FAK siRNA: 0.55 ± 0.08, $P < .001$; Erk1 siRNA: 0.56 ± 0.07, $P < .001$; FAK+Erk1 siRNA: 0.77 ± 0.22, $P = .16$) (Figure 6E). Intriguingly, radiation survival remained unchanged under single Erk1 (surviving fraction 6 Gy: 0.22 ± 0.09, $P = .67$) and concomitant FAK/Erk1 (surviving fraction 6 Gy: 0.15 ± 0.06, $P = .72$) depletion, while silencing of FAK (surviving fraction 6 Gy: 0.07 ± 0.04, $P = .07$) alone

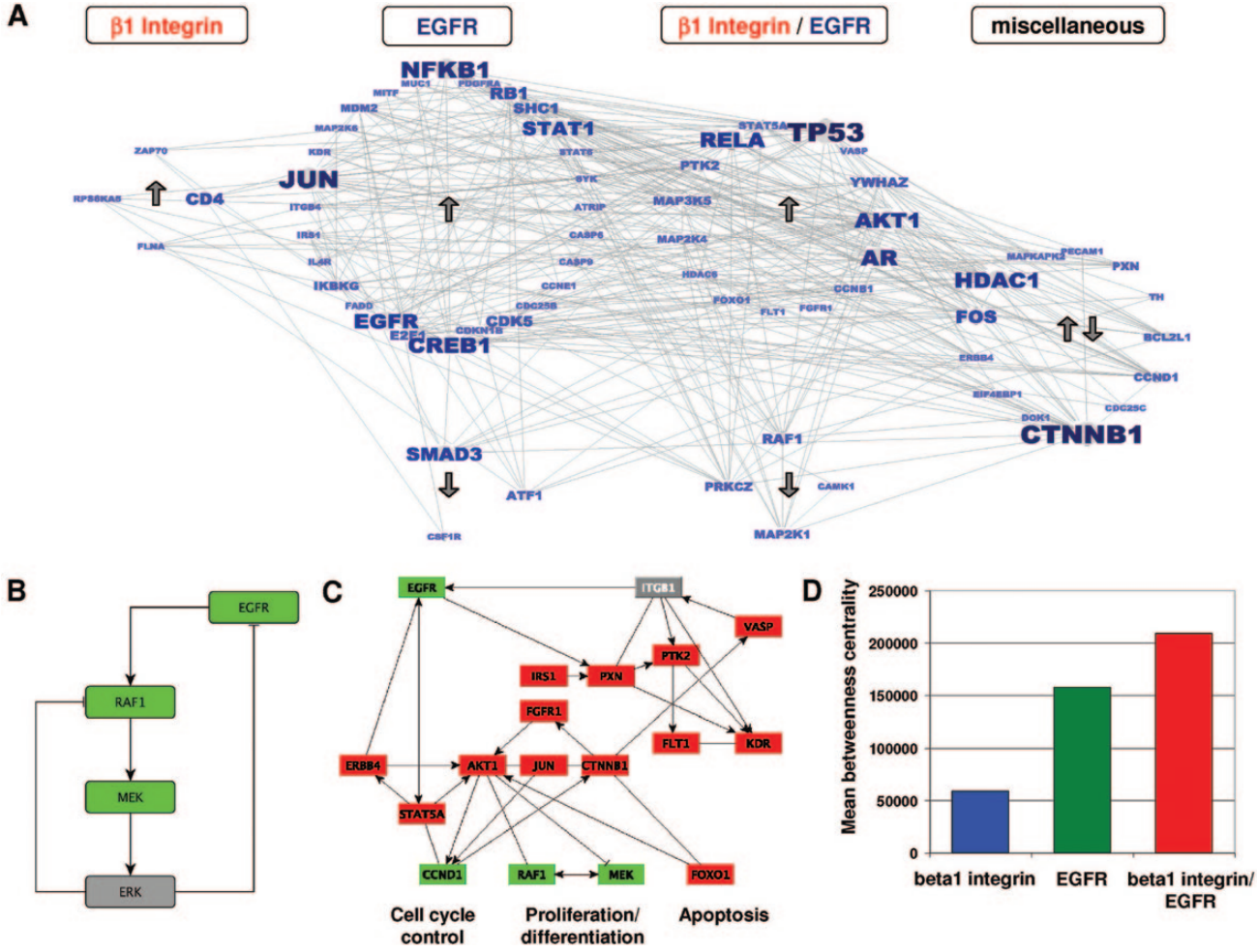

Figure 4. Interactome analysis of deregulated phosphoproteins after single and combined inhibition of β1 integrin and epidermal growth factor receptor (EGFR). **A)** Deregulated phosphoproteins after single and combined inhibition of β1 integrin and EGFR were mapped to the Reactome Functional Interaction (FI) network, and the nodes (phosphoproteins) were arranged according to their specific deregulation after inhibition of β1 integrin (**left**), EGFR (**second from left**), or EGFR/β1 integrin (**second from right**). Phosphoproteins that are not specifically allocated to either β1 integrin or EGFR signaling were categorized "miscellaneous" (**right**). Phosphosites were considered as differentially expressed if the expressions in the samples deviated from the averaged expressions in the controls by a factor of 2 (>2 upregulation, <0.5 downregulation). Downregulated phosphoproteins are grouped around **down arrows** and upregulated phosphoproteins around **up arrows**. The "miscellaneous" group contains both up- and downregulated phosphoproteins. The font size and the intensity of the font color of each node are proportional to their log10-transformed betweeness centrality (BC) values. BC is a measure calculated for each node separately and is the number of shortest connections from all nodes to all others in the network that pass through that node. The higher the BC, the more central/important is the node for the network. **B)** Negative feedback EGFR/Raf/MEK/Erk that is specifically broken in the double-treated cells leading to subsequent downregulation of EGFR. **Green** node color indicates downregulation. The expression of Erk (**gray**) was not determined. **C)** Network representation of phosphoproteins up- (**red**) and downregulated (**green**) in the focal adhesion pathway after double inhibition of EGFR and β1 integrin. **D)** Barplots of the mean BC of the three treatment groups. EGFR = epidermal growth factor receptor.

mediated radiosensitization (Figure 6F). In line with previous reports (33,43), these data suggest profound roles of FAK and Erk1 in HNSCC cell survival, with Erk1 being unable to compensate for FAK in case of genotoxic stress; thus, FAK plays a fundamental role downstream of Erk1 in this protein complex and for the cellular DNA damage survival response (Figure 6G).

Discussion

Our study shows that simultaneous targeting of β1 integrin and EGFR for radiosensitization is superior to monotargeting in preclinical HNSCC models. Based on dephosphorylated FAK and hyperphosphorylated Erk1/2, we differentiated between β1 integrin/EGFR therapy responders and nonresponders. Mechanistically, a protein complex formed by FAK and Erk1 channels prosurvival signals for radioresistance, which is effectively impaired by combined β1 integrin/EGFR blocking.

Therapy resistance in cancer remains one of the most challenging obstacles to overcome. Both preclinically and clinically, multitargeting approaches with selective agents are rare and could effectively inhibit a broader part of the prosurvival signaling network. Moreover, the dynamic and elusive nature of cancer cell resistance processes and the difficulty to practically translate the multitargeting concept into the clinic in respect of patient morbidity and adverse, therapy-confining normal tissue effects requires consideration (54,55). Additionally, drug efficacy might be a cell population–dependent addiction on a specific oncogene, essentially determining the susceptibility of the tumor to a targeted drug (56). Obviously, our work points at a discrimination between responder and nonresponder tumor models in the order of several magnitudes, which is highly likely to originate from specific intrinsic, subpopulation-independent phenotypes and not from differential β1 integrin or EGFR expression. For personalization, a clinically manageable approach

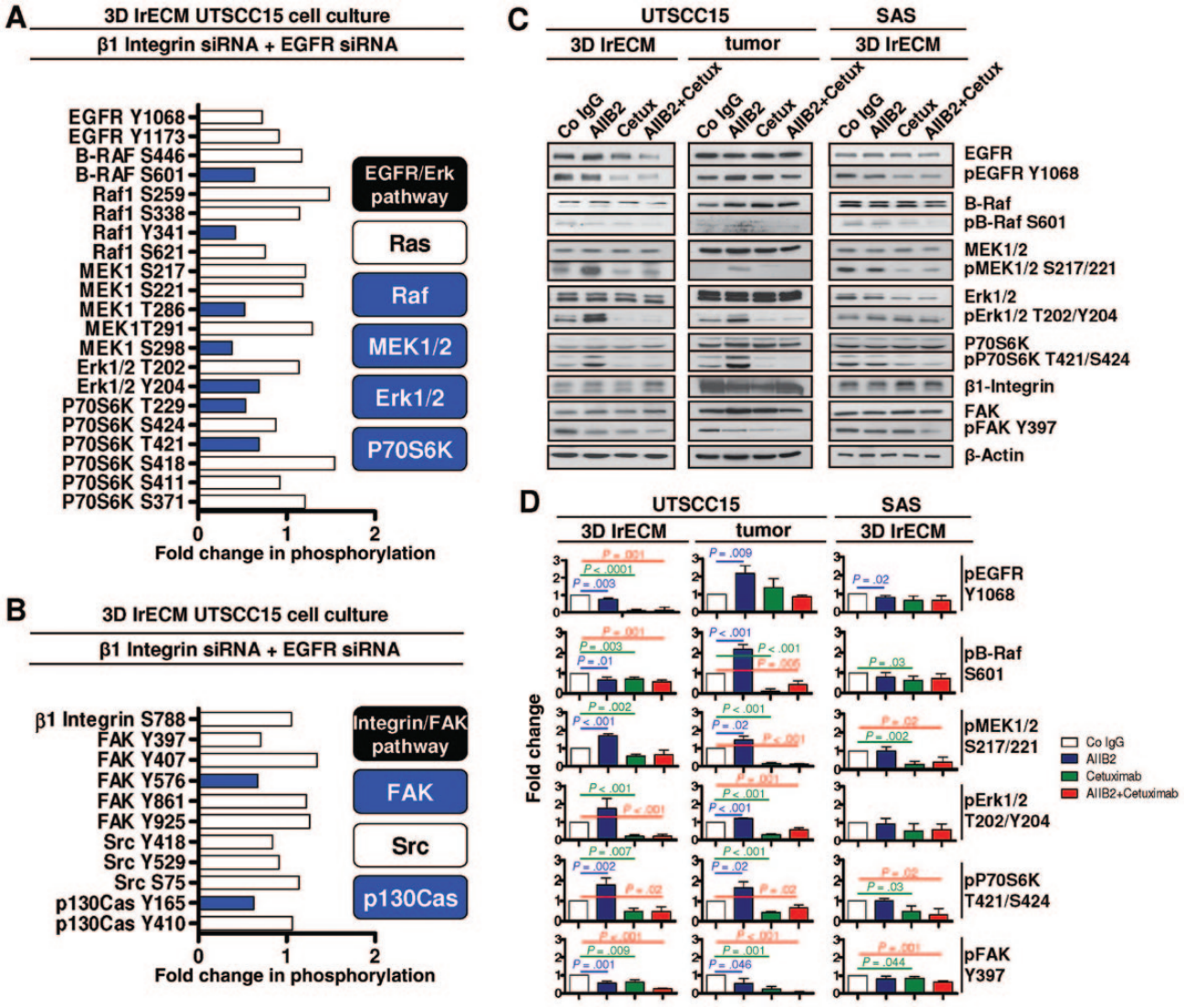

Figure 5. Combined AIIB2 and cetuximab treatment prevents AIIB2-mediated activation of the MEK/ERK pathway. Phosphoproteome array–based analysis of **(A)** epidermal growth factor receptor (EGFR) pathway and **(B)** β1 integrin pathway on whole cell lysates of 3D UTSCC15 cell cultures after double knockdown of β1 integrin and EGFR-nonspecific siRNA as control. Data are presented as fold change to nonspecific siRNA controls after normalization to total protein expression. **C)** Western blotting and **(D)** densitometric analysis of 3D-cultured UTSCC15 and SAS cell cultures (in vitro) or UTSCC15 xenografts (in vivo) after indicated treatment (mean ± SD, $n = 3$, two-sided t test). EGFR = epidermal growth factor receptor; lrECM = laminin-rich extracellular matrix.

would test for FAK dephosphorylation on fresh patient tumor specimens exposed to AIIB2/cetuximab.

The rationale for an AIIB2/cetuximab combination arose from the detection of prosurvival bypass signaling induced by β1 integrin inhibition. Despite strong radiosensitization, β1 integrin blocking stimulated B-Raf-MEK1/2-Erk1/2 signaling generally associated with cell proliferation and improved survival (57). Intriguingly, negative feedback loops including MEK1/2 and other bypass signaling have been reported for anti-EGFR therapeutics like cetuximab and Erlotinib (17,18,58,59) to be, at least partly, β1 integrin-dependent (18,58). Conversely, our data demonstrate activated EGFR-associated signaling as a consequence of β1 integrin inhibition, thus indicating cooperative and mutual EGFR/β1 integrin interaction (16,18,26,27,43). As radiotherapy plus cetuximab represents one of the first-line treatment options for HNSCC (Cisplatin was not considered here) (8), we exploited simultaneous β1 integrin/EGFR deactivation for pinpointing the clinical potential of such an approach together with radiotherapy.

Mechanistically, bioinformatics on phosphoproteome data for interactome and network betweeness centrality plus the endpoint of DSB repair provided some explanation for the variation in responsiveness to AIIB2/cetuximab in the different HNSCC models. The bioinformatics fundamentally illustrated that the observed radiosensitization through β1 integrin/EGFR targeting results from an extensive cytoplasmic and nuclear signaling network deactivation. Interestingly, mathematical modeling to uncover suitable multitargeting solutions for anti-EGFR agents also revealed B-Raf-MEK cascade as one possible intervention point (59). One consequence was the increased DSB rate, suggesting a critical function of β1 integrin and EGFR in DNA damage repair. While nuclear EGFR interactions with DNA-PK for nonhomologous end joining and via Rad51 for homologous recombination (60–62) are known, β1 integrins have received less attention in this context. They seem to participate in chromatin organization through histone H3 acetylation, reduced linker histone H1-DNA association (63) and bleomycin-induced

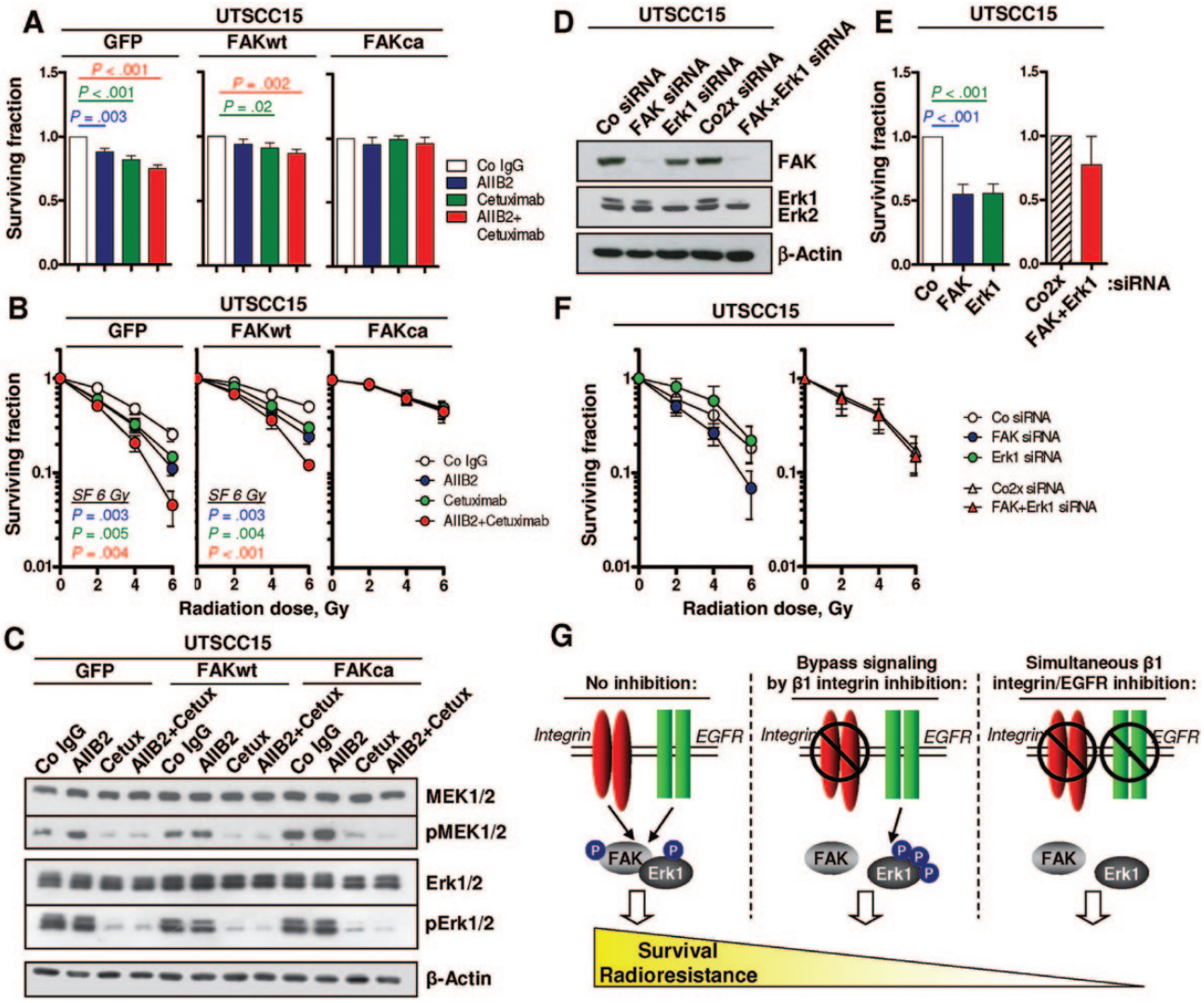

Figure 6. Constitutively active focal adhesion kinase (FAK) abrogates radiosensitization caused by β1 integrin and EGFR inhibition. **A)** Basal cell survival and **(B)** radiosensitivity of UTSCC15 cells stably transfected with wildtype FAK-GFP (FAKwt), constitutively active FAK-GFP (FAKca, K578E/K581E) and GFP empty vector controls (GFP). Cells were treated with AIIB2 and/or cetuximab 24 hours prior to x-ray irradiation (2–6 Gy) (mean ± SD, n = 3, two-sided *t* test). *P* values compare surviving fractions (SF) after 6 Gy upon treatment with AIIB2 vs control IgG (**blue**), cetuximab vs control IgG (**green**), or AIIB2 plus cetuximab vs control IgG (**red**). **C)** Western blotting from whole cell lysates of UTSCC15 cells stably transfected with FAK-GFP fusion constructs. Cells were treated with AIIB2 and/or cetuximab for one hour. β-Actin served as loading control. **D)** Western blot, **E)** basal survival, and **F)** radiation survival of 3D-grown UTSCC15 cells after knockdown of FAK plus/minus Erk1. Nonspecific siRNA (Co siRNA) was used as control (mean ± SD, n = 3, two-sided *t* test). **G)** Schematic of how inhibition of β1 integrin results in activation of the EGFR pathway and additional targeting of EGFR increases radiosensitization in human head and neck squamous cell carcinomas. EGFR = epidermal growth factor receptor.

base excision repair (64). In contrast to EGFR with intrinsic kinase activity, the integrin-mediated regulations rely on signaling mediators, of which FAK is one of the most prominent ones. Its key role became obvious by abrogating AIIB2 and cetuximab effects when its kinase was constitutively active (FAKca transfectants). Based on the similarity in FAKca and nonresponder SAS cell behavior, we hypothesize similar underlying, yet-to-be-identified mechanisms, which might be exploitable to overcome the nonsusceptibility for β1 integrin and EGFR targeting. As a next important step for a bench-to-bedside translation, a comprehensive comparative characterization of the molecular phenotype of responder vs nonresponder tumor models is required. The identified molecular signature with robust biomarkers and a clinically applicable predictive assay should then enable the stratification of patients for simultaneous β1 integrin/EGFR targeting and radiotherapy.

By exploring the hierarchical localization of FAK, MEK1/2, and Erk1/2, we found MEK1/2 and Erk1/2 dephosphorylation occurring FAK independently, which stresses the position of FAK to be downstream of MEK1/2-Erk1/2. In human ovarian cancer cells (65), lung cancer cells (26), and HNSCC cells (43), FAK has been shown to channel downstream to MEK1/2-Erk1/2 as part of the same signaling axis (39,40). Hence, these surprising findings suggest profound roles of both FAK and Erk1 in clonogenic cell survival. As Erk1 seems incompetent to compensate for FAK, FAK plays a fundamental role downstream of Erk1 in the FAK-Erk1 protein complex and for the cellular DNA damage survival response.

This is, to our knowledge, the first study to demonstrate the efficacy and feasibility of simultaneous β1 integrin/EGFR targeting in combination with radiotherapy in HNSCC tumor xenografts and 3D matrix–based HNSCC cell cultures. Owing to

frequent overexpression of β1 integrins and EGFR in cancer, the presented strategy can be envisioned for additional tumor entities originating from lung, pancreas, brain, and breast. Whether the cross susceptibility between anti-β1 integrin (AIIB2) and anti-EGFR (cetuximab) agents seen in HNSCC is observable in other tumor types and associated with similar efficacy remains to be elucidated. The limitation of this study is that the normal tissue effects conferred by cetuximab could not be evaluated because of the chimeric nature of this antibody, a circumstance not applicable to AIIB2 (66). In conclusion, combined β1 integrin/EGFR inhibition plus irradiation statistically significantly improves tumor control and might be a reasonable and efficient treatment option to overcome tumor radioresistance and diminish tumor recurrence in patients.

Funding

The work was in part supported by a grant from the Bundesministerium für Bildung und Forschung (BMBF Contracts 03ZIK041 and BMBF-02NUK006B to NC), the Deutsche Krebshilfe e.V. (grant number 110834 to NC), the EFRE Europäische Fonds für regionale Entwicklung, Europa fördert Sachsen (grant number 100066308 to NC), the Deutsche Forschungsgemeinschaft (grant number Ba1433/5 to MK), and the Medizinische Fakultät Carl Gustav Carus, Technische Universität Dresden, Germany (MeDDrive grant to IE).

Notes

We thank D. D. Schlaepfer for reagents, R. Grenman for cell lines, I. Lange, L. Stolz-Kieslich, and K. Schumann for excellent technical assistance. We are grateful to E. Hammond for critically reading the manuscript. All authors discussed the results, commented on the manuscript, and approved the final manuscript. IE, MK, and NC conceived and designed the experiments. IE, KZ, ED, EM, and LH performed the experiments and analyzed the data. KU performed bioinformatics. IE, KZ, MK, KU, and NC wrote the manuscript. The study sponsors did not have any role in the design of the study, the collection, analysis or interpretation of the data, the writing of the article, nor the decision to submit the article for publication.

The authors have no conflicts of interest to declare.

References

1. Hanahan D, Weinberg RA. Hallmarks of cancer: the next generation. *Cell*. 2010;144(5):646–674.
2. Tredan O, Galmarini CM, Patel K, Tannock IF. Drug resistance and the solid tumor microenvironment. *J Natl Cancer Inst*. 2007;99(19):1441–1454.
3. Burrell RA, McGranahan N, Bartek J, Swanton C. The causes and consequences of genetic heterogeneity in cancer evolution. *Nature*. 2013;501(7467):338–345.
4. Gerber DE, Minna JD. ALK inhibition for nonsmall cell lung cancer: from discovery to therapy in record time. *Cancer Cell*. 2011;18(6):548–551.
5. Krause M, Gurtner K, Deuse Y, Baumann M. Heterogeneity of tumour response to combined radiotherapy and EGFR inhibitors: differences between antibodies and TK inhibitors. *Int J Radiat Biol*. 2009;85(11):943–954.
6. Sawyers C. Targeted cancer therapy. *Nature*. 2004;432(7015):294–297.
7. Lin SH, George TJ, Ben-Josef E, et al. Opportunities and challenges in the era of molecularly targeted agents and radiation therapy. *J Natl Cancer Inst*. 2013;105(10):686–693.
8. Bonner JA, Harari PM, Giralt J, et al. Radiotherapy plus cetuximab for locoregionally advanced head and neck cancer: 5-year survival data from a phase 3 randomised trial, and relation between cetuximab-induced rash and survival. *Lancet Oncol*. 2010;11(1):21–28.
9. Damiano JS. Integrins as novel drug targets for overcoming innate drug resistance. *Curr Cancer Drug Targets*. 2002;2(1):37–43.
10. Desgrosellier JS, Cheresh DA. Integrins in cancer: biological implications and therapeutic opportunities. *Nat Rev Cancer*. 2010;10(1):9–22.
11. Hehlgans S, Haase M, Cordes N. Signalling via integrins: implications for cell survival and anticancer strategies. *Biochim Biophys Acta*. 2007;1775(1):163–180.
12. Weaver VM, Lelievre S, Lakins JN, et al. beta4 integrin-dependent formation of polarized three-dimensional architecture confers resistance to apoptosis in normal and malignant mammary epithelium. *Cancer Cell*. 2002;2(3):205–216.
13. Shin DH, Lee HJ, Min HY, et al. Combating resistance to anti-IGFR antibody by targeting the integrin beta3-Src pathway. *J Natl Cancer Inst*. 2013;105(20):1558–1570.
14. Hynes NE, MacDonald G. ErbB receptors and signaling pathways in cancer. *Curr Opin Cell Biol*. 2009;21(2):177–184.
15. Gurtner K, Deuse Y, Butof R, et al. Diverse effects of combined radiotherapy and EGFR inhibition with antibodies or TK inhibitors on local tumour control and correlation with EGFR gene expression. *Radiother Oncol*. 2011;99(3):323–330.
16. Eke I, Cordes N. Dual targeting of EGFR and focal adhesion kinase in 3D grown HNSCC cell cultures. *Radiother Oncol*. 2011;99(3):279–286.
17. Eke I, Schneider L, Forster C, Zips D, Kunz-Schughart LA, Cordes N. EGFR/JIP-4/JNK2 signaling attenuates cetuximab-mediated radiosensitization of squamous cell carcinoma cells. *Cancer Res*. 2013;73(1):297–306.
18. Eke I, Storch K, Krause M, Cordes N. cetuximab Attenuates Its Cytotoxic and Radiosensitizing Potential by Inducing Fibronectin Biosynthesis. *Cancer Res*. 2013;73(19):5869–5879.
19. Jackman D, Pao W, Riely GJ, et al. Clinical definition of acquired resistance to epidermal growth factor receptor tyrosine kinase inhibitors in nonsmall-cell lung cancer. *J Clin Oncol*. 2010;28(2):357–360.
20. Yatabe Y, Takahashi T, Mitsudomi T. Epidermal growth factor receptor gene amplification is acquired in association with tumor progression of EGFR-mutated lung cancer. *Cancer Res*. 2008;68(7):2106–2111.
21. Wheeler DL, Dunn EF, Harari PM. Understanding resistance to EGFR inhibitors-impact on future treatment strategies. *Nat Rev Clin Oncol*. 2010;7(9):493–507.
22. Shepard HM, Brdlik CM, Schreiber H. Signal integration: a framework for understanding the efficacy of therapeutics targeting the human EGFR family. *J Clin Invest*. 2008;118(11):3574–3581.
23. Yamada KM, Even-Ram S. Integrin regulation of growth factor receptors. *Nat Cell Biol*. 2002;4(4):E75–E76.
24. Siena S, Sartore-Bianchi A, Di Nicolantonio F, Balfour J, Bardelli A. Biomarkers predicting clinical outcome of epidermal growth factor receptor-targeted therapy in metastatic colorectal cancer. *J Natl Cancer Inst*. 2009;101(19):1308–1324.
25. Petras M, Lajtos T, Friedlander E, et al. Molecular interactions of ErbB1 (EGFR) and integrin-beta1 in astrocytoma frozen sections predict clinical outcome and correlate with Akt-mediated in vitro radioresistance. *Neuro Oncol*. 2013;15(8):1027–1040.
26. Morello V, Cabodi S, Sigismund S, et al. beta1 integrin controls EGFR signaling and tumorigenic properties of lung cancer cells. *Oncogene*. 2011;30(39):4087–4096.
27. Moro L, Venturino M, Bozzo C, et al. Integrins induce activation of EGF receptor: role in MAP kinase induction and adhesion-dependent cell survival. *Embo J*. 1998;17(22):6622–6632.

28. Eriksen JG, Steiniche T, Sogaard H, Overgaard J. Expression of integrins and E-cadherin in squamous cell carcinomas of the head and neck. *Apmis*. 2004;112(9):560–568.
29. Yao ES, Zhang H, Chen YY, et al. Increased beta1 integrin is associated with decreased survival in invasive breast cancer. *Cancer Res*. 2007;67(2):659–664.
30. Janes SM, Watt FM. New roles for integrins in squamous-cell carcinoma. *Nat Rev Cancer*. 2006;6(3):175–183.
31. Cordes N, Seidler J, Durzok R, Geinitz H, Brakebusch C. beta1-integrin-mediated signaling essentially contributes to cell survival after radiation-induced genotoxic injury. *Oncogene*. 2006;25(9):1378–1390.
32. Park CC, Zhang HJ, Yao ES, Park CJ, Bissell MJ. Beta1 integrin inhibition dramatically enhances radiotherapy efficacy in human breast cancer xenografts. *Cancer Res*. 2008;68(11):4398–4405.
33. Eke I, Deuse Y, Hehlgans S, et al. beta(1)Integrin/FAK/cortactin signaling is essential for human head and neck cancer resistance to radiotherapy. *J Clin Invest*. 2012;122(4):1529–1540.
34. Hynes RO. Integrins: bidirectional, allosteric signaling machines. *Cell*. 2002;110(6):673–687.
35. Moser M, Legate KR, Zent R, Fassler R. The tail of integrins, talin, and kindlins. *Science*. 2009;324(5929):895–899.
36. Shibue T, Weinberg RA. Integrin beta1-focal adhesion kinase signaling directs the proliferation of metastatic cancer cells disseminated in the lungs. *Proc Natl Acad Sci U S A*. 2009;106(25):10290–10295.
37. Vehlow A, Cordes N. Invasion as target for therapy of glioblastoma multiforme. *Biochim Biophys Acta*. 2013;1836(2):236–244.
38. Legate KR, Fassler R. Mechanisms that regulate adaptor binding to beta-integrin cytoplasmic tails. *J Cell Sci*. 2009;122(Pt 2):187–198.
39. Cance WG, Kurenova E, Marlowe T, Golubovskaya V. Disrupting the scaffold to improve focal adhesion kinase-targeted cancer therapeutics. *Sci Signal*. 2013;6(268):pe10.
40. Mitra SK, Schlaepfer DD. Integrin-regulated FAK-Src signaling in normal and cancer cells. *Curr Opin Cell Biol*. 2006;18(5):516–523.
41. Lim ST, Mikolon D, Stupack DG, Schlaepfer DD. FERM control of FAK function: implications for cancer therapy. *Cell Cycle*. 2008;7(15):2306–2314.
42. Sood AK, Armaiz-Pena GN, Halder J, et al. Adrenergic modulation of focal adhesion kinase protects human ovarian cancer cells from anoikis. *J Clin Invest*. 2010;120(5):1515–1523.
43. Hehlgans S, Eke I, Cordes N. Targeting FAK radiosensitizes 3-dimensional grown human HNSCC cells through reduced Akt1 and MEK1/2 signaling. *Int J Radiat Oncol Biol Phys*. 2012;83(5):e669–e676.
44. Yuan Z, Zheng Q, Fan J, Ai KX, Chen J, Huang XY. Expression and prognostic significance of focal adhesion kinase in hepatocellular carcinoma. *J Cancer Res Clin Oncol*. 2010;136(10):1489–1496.
45. Cance WG, Harris JE, Iacocca MV, et al. Immunohistochemical analyses of focal adhesion kinase expression in benign and malignant human breast and colon tissues: correlation with preinvasive and invasive phenotypes. *Clin Cancer Res*. 2000;6(6):2417–2423.
46. Owens LV, Xu L, Craven RJ, et al. Overexpression of the focal adhesion kinase (p125FAK) in invasive human tumors. *Cancer Res*. 1995;55(13):2752–2755.
47. Eke I, Koch U, Hehlgans S, et al. PINCH1 regulates Akt1 activation and enhances radioresistance by inhibiting PP1alpha. *J Clin Invest*. 2010;120(7):2516–2527.
48. Storch K, Eke I, Borgmann K, et al. Three-dimensional cell growth confers radioresistance by chromatin density modification. *Cancer Res*. 2010;70(10):3925–3934.
49. Gabarra-Niecko V, Keely PJ, Schaller MD. Characterization of an activated mutant of focal adhesion kinase: 'SuperFAK'. *Biochem J*. 2002;365(Pt 3):591–603.
50. Matthews L, Gopinath G, Gillespie M, et al. Reactome knowledgebase of human biological pathways and processes. *Nucleic Acids Res*. 2009;37(Database issue):D619–D622.
51. Cline MS, Smoot M, Cerami E, et al. Integration of biological networks and gene expression data using Cytoscape. *Nat Protoc*. 2007;2(10):2366–2382.
52. Kanehisa M, Goto S. KEGG: kyoto encyclopedia of genes and genomes. *Nucleic Acids Res*. 2000;28(1):27–30.
53. Unger K. Integrative radiation systems biology. *Radiat Oncol*. 2014;9:21.
54. Hu X, Xuan Y. Bypassing cancer drug resistance by activating multiple death pathways--a proposal from the study of circumventing cancer drug resistance by induction of necroptosis. *Cancer Lett*. 2008;259(2):127–137.
55. Yano S, Takeuchi S, Nakagawa T, Yamada T. Ligand-triggered resistance to molecular targeted drugs in lung cancer: roles of hepatocyte growth factor and epidermal growth factor receptor ligands. *Cancer Sci*. 2012;103(7):1189–1194.
56. Tsai CJ, Nussinov R. The molecular basis of targeting protein kinases in cancer therapeutics. *Semin Cancer Biol*. 2013;23(4):235–242.
57. Mebratu Y, Tesfaigzi Y. How ERK1/2 activation controls cell proliferation and cell death: Is subcellular localization the answer? *Cell Cycle*. 2009;8(8):1168–1175.
58. Kanda R, Kawahara A, Watari K, et al. Erlotinib resistance in lung cancer cells mediated by integrin beta1/Src/Akt-driven bypass signaling. *Cancer Res*. 2013;73(20):6243–6253.
59. Klinger B, Sieber A, Fritsche-Guenther R, et al. Network quantification of EGFR signaling unveils potential for targeted combination therapy. *Mol Syst Biol*. 2013;9:673.
60. Wang Y, Yuan JL, Zhang YT, et al. Inhibition of both EGFR and IGF1R sensitized prostate cancer cells to radiation by synergistic suppression of DNA homologous recombination repair. *PLoS One*. 2013;8(8):e68784.
61. Huang S, Benavente S, Armstrong EA, Li C, Wheeler DL, Harari PM. p53 modulates acquired resistance to EGFR inhibitors and radiation. *Cancer Res*. 2011;71(22):7071–7079.
62. Dittmann K, Mayer C, Fehrenbacher B, et al. Radiation-induced epidermal growth factor receptor nuclear import is linked to activation of DNA-dependent protein kinase. *J Biol Chem*. 2005;280(35):31182–31189.
63. Rose JL, Huang H, Wray SF, Hoyt DG. Integrin engagement increases histone H3 acetylation and reduces histone H1 association with DNA in murine lung endothelial cells. *Mol Pharmacol*. 2005;68(2):439–446.
64. Rose JL, Reeves KC, Likhotvorik RI, Hoyt DG. Base excision repair proteins are required for integrin-mediated suppression of bleomycin-induced DNA breakage in murine lung endothelial cells. *J Pharmacol Exp Ther*. 2007;321(1):318–326.
65. Rea K, Sensi M, Anichini A, Canevari S, Tomassetti A. EGFR/MEK/ERK/CDK5-dependent integrin-independent FAK phosphorylated on serine 732 contributes to microtubule depolymerization and mitosis in tumor cells. *Cell Death Dis*. 2013;4:e815.
66. Albert M, Schmidt M, Cordes N, Dorr W. Modulation of radiation-induced oral mucositis (mouse) by selective inhibition of beta1 integrin. *Radiother Oncol*. 2012;104(2):230–234.